SpaC and NisC, the Cyclases Involved in Subtilin and Nisin Biosynthesis, Are Zinc Proteins†

Nicole M. Okeley,‡ Moushumi Paul,‡ Jay P. Stasser,§ Ninian Blackburn,*,§ and Wilfred A. van der Donk*,‡

Department of Chemistry, University of Illinois at Urbana−Champaign, 600 South Mathews Avenue, Urbana, Illinois 61801, and Department of Biochemistry and Molecular Biology, OGI School of Science and Engineering at OHSU, 20000 Northwest Walker Road, Beaverton, Oregon 97006-8921

Received August 20, 2003

ABSTRACT: Lantibiotics are peptide-derived antimicrobial agents that are ribosomally synthesized and posttranslationally modified by a multienzyme complex to their biologically active forms. Nisin has attracted much attention recently due to its novel mechanism of action including specific binding to the bacterial cell wall precursor lipid II, followed by membrane permeabilization. Nisin has been commercially used as a food preservative, while other lantibiotics show promising activity against bacterial infections. The posttranslational modifications are believed to be carried out by a multienzyme complex. At present the enzymes catalyzing the formation of the lantibiotic signature structural motifs, dehydroalanine (Dha), dehydrobutyrine (Dhb), lanthionine (Ln), and methyllanthionine (MeLn), are poorly characterized. In an effort to gain insight into the mechanism by which lantibiotics are biosynthesized, the cyclase enzymes involved in the synthesis of nisin and subtilin (NisC and SpaC, respectively) have been cloned, expressed, and purified. Both proteins exist as monomers in solution and contain a stoichiometric zinc atom. EXAFS data on SpaC and a C349A mutant are in line with two cysteine ligands to the metal in the wild-type enzyme with possibly two additional histidines. The two cysteine ligands are likely Cys303 and Cys349 on the basis of sequence alignments and EXAFS data. The metal may function to activate the cysteine thiol of the peptide substrate toward intramolecular Michael addition to the dehydroalanine and dehydrobutyrine residues in the peptide.

Nisin and subtilin are pentacyclic, posttranslationally modified peptides that belong to the lantibiotic family of bacteriocins. Lantibiotics possess high antimicrobial activity against Gram-positive bacteria, including staphylococci, streptococci, and clostridia, and have been used for a variety of applications including food preservation (*1*, *2*). Their unique structural motifs, including dehydroalanine (Dha), dehydrobutyrine (Dhb), lanthionine (Ln), and methyllanthionine (MeLn, Figure 1), are responsible for their biological activity and are the basis for their adopted family name (*2*, *3*). These unusual structures are introduced posttranslationally into a ribosomally synthesized peptide by a multienzyme complex. Nisin and subtilin owe their bactericidal activity to the depolarization of energized cell membranes through pore formation. Nisin is effective at concentrations that are several orders of magnitude lower than many other pore-forming antibacterial agents and is significantly more potent toward Gram-positive intact cells than liposomes. This unusual profile was recently explained by the observation

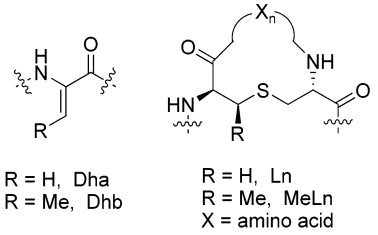

FIGURE 1: Four characteristic structural motifs found in lantibiotics.

that nisin initially associates with membrane-bound lipid II, an intermediate in cell wall biosynthesis (*6*−*8*).

A number of open reading frames surrounding the lantibiotic structural genes have been sequenced. Putative roles have been assigned to each protein ranging from biosynthesis, transport, and regulation to immunity against lantibiotics. The LanB,[1] LanC, and LanP proteins are thought to be involved in biosynthesis of the mature products (*2*). After ribosomal production of the prepeptide, LanB-catalyzed dehydration

† This work was supported by grants from the National Institutes of Health to W.A.v.d.D. (GM58822) and N.B. (GM54803). N.M.O. thanks Abbott Laboratories for a predoctoral fellowship. W.A.v.d.D. is a Cottrell Scholar of the Research Corporation and an Alfred P. Sloan Fellow.

* To whom correspondence should be addressed. W.A.v.d.D.: phone, 217-244-5360; fax, 217-244-8068; e-mail, vddonk@uiuc.edu. N.B.: phone, 503-748-1384; e-mail, ninian@bmb.ogi.edu.

‡ University of Illinois at Urbana−Champaign.

§ OGI School of Science and Engineering at OHSU.

[1] Abbreviations: ATCC, American Type Culture Collection; BVS, bond valence sum; DEAE, (diethylamino)ethyl; Dha, dehydroalanine; Dhb, dehydrobutyrine; DTNB, 5,5′-dithiobis(2-nitrobenzoic acid); DTT, dithiothreitol; DW, Debye−Waller; ESI, electrospray ionization; EXAFS, extended X-ray absorption fine structure; Gdn-HCl, guanidine hydrochloride; ICP-MS, inductively coupled plasma mass spectrometry; LanB, lantibiotic dehydratase enzymes; LanC, lantibiotic cyclase enzymes; LanP, lantibiotic serine proteases; Ln, lanthionine; MALDI, matrix-assisted laser desorption ionization; MeLn, methyllanthionine; MMTS, methyl methanethiosulfonate; PAR, 4-(2-pyridylazo)resorcinol; SPPS, solid phase peptide synthesis; TCEP, tris(carboxyethyl)phosphine.

10.1021/bi0354942 CCC: $25.00
Published on Web 10/30/2003

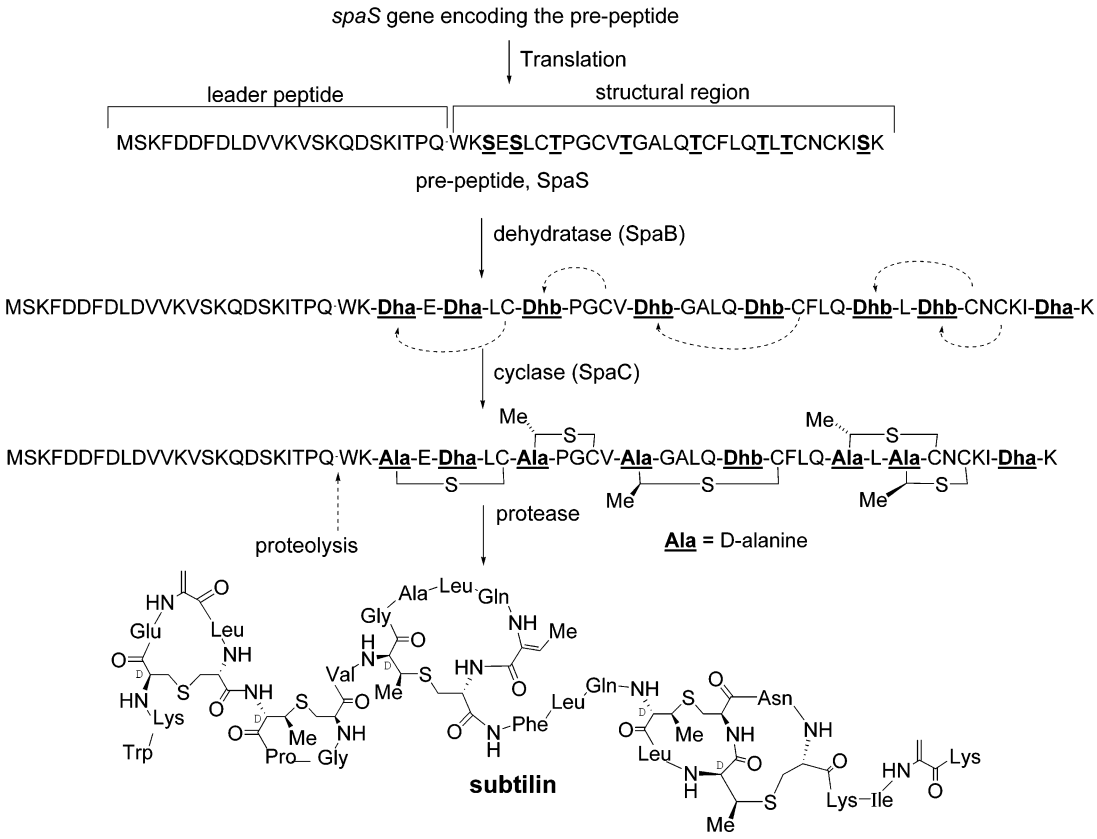

FIGURE 2: Proposed biosynthetic pathway for subtilin.

of serine and threonine residues in the C-terminal region putatively generates multiple Dha and Dhb residues, respectively (e.g., Figure 2 for subtilin). In the second step, the LanC enzymes are thought to mediate the regio- and stereoselective cyclization of cysteine residues onto these dehydroamino acids to assemble the thioether ring structures (*9*). In some lantibiotic-producing organisms, the LanB and LanC proteins are absent, and a single protein, LanM having homology to the LanC enzymes at its C-terminus, is produced instead (*10*, *11*). These LanM proteins are postulated to carry out both dehydration and cyclization reactions. In the ultimate step, the unmodified N-terminal leader sequence is proteolytically removed by LanP to yield the mature, active lantibiotic.

Nisin is produced by *Lactococcus lactis* and has been used as a biopreservative for over 30 years (*12*). Subtilin, produced by *Bacillus subtilis*, possesses 63% sequence identity to nisin (*13*), including the presence of lanthionine and methyllanthionine rings of identical size and relative position (Figure 2). The biosynthetic genes for the production of both compounds have been completely sequenced (*14*, *15*). The putative dehydratases SpaB and NisB have been overexpressed (*16*, *17*), but the cyclases NisC and SpaC have received little attention. The homologous proteins EpiC and PepC involved in the production of the lantibiotics epidermin and Pep5 have been purified, but their activity could not be tested due to the absence of a dehydrated peptide substrate (*18*, *19*). As part of our efforts to understand the biosynthesis of lantibiotics (*17*, *20*−*22*), we have undertaken the task of cloning, overexpressing, and purifying the two cyclase enzymes involved in subtilin and nisin biosynthesis, SpaC and NisC. We show here that both proteins are monomers in solution and contain a stoichiometric zinc. The metal coordination environment of SpaC was investigated by EXAFS. Our results suggest that these proteins may be members of a growing family of proteins that utilize zinc for activation of thiol substrates.

MATERIALS AND METHODS

Materials. The lantibiotic-producing strains *L. lactis* 11454 and *B. subtilis* 6633 were obtained from the American Type Culture Collection. Chemically competent *Escherichia coli* DH5α cells (subcloning efficiency) were purchased from GibcoBRL, and media were purchased from Difco laboratories. Oligonucleotide primers were synthesized by Operon Technologies, and cloned Pfu polymerase was obtained from Stratagene. Deoxyribonucleotides and T4 DNA ligase were purchased from either Boehringer Mannheim or GibcoBRL. Restriction enzymes and proteinase K were from GibcoBRL, and calf intestinal alkaline phosphatase was provided by Promega. The QuikChange site-directed mutagenesis kit was purchased from Stratagene. Tris(hydroxymethyl)aminomethane (Tris, Fisher) buffer contained 20 mM Tris, pH 7.5 at 4 °C. TE buffer contained 10 mM Tris, 1 mM EDTA, and 0.08% Triton X-100, pH 7.5.

General Methods. Molecular biological manipulations were carried out using standard techniques (*23*). Cell disruption was performed with a Sonics and Materials Vibra Cell model sonicator. Protein purification was accomplished by column chromatography using either peristaltic pumps from Pharmacia Biotech or a BioCAD purification system from PerSeptive Biosystems. Mass spectrometry was performed by the Mass Spectrometry Laboratory at the University of Illinois using electrospray ionization (ESI) or matrix-assisted laser desorption ionization (MALDI). Protein

concentrations were determined using both the biuret or Bradford methods using bovine serum albumin as standard; the values obtained with both methods were in close agreement (±5%) and were also consistent (±8%) with values determined using a theoretical molar absorptivity constant extinction coefficient calculated on the basis of amino acid content. Using the Lowry assay provided values that were somewhat different from the other three methods and resulted in protein concentrations that were higher by 1.3-fold. All metal and thiol content values reported herein are based on the values determined by the Bradford assay. Automated peptide synthesis was performed on a Rainin Model PS3 peptide synthesizer. RP-HPLC was performed on a Rainin system (Dynamax Model SD-200 pump and Model UV-1 detector).

Construction of Overexpression Plasmids. *B. subtilis* ATCC 6633 was grown in TY medium (0.8% tryptone, 0.5% yeast extract, 0.1% glucose, and 0.5% NaCl). *L. lactis* ATCC 11454 was grown in M17 broth supplemented with 0.5% glucose. The genomic DNA of *B. subtilis* was purified by harvesting the cells at 4750*g* for 10 min followed by resuspension in TE buffer and boiling for 5 min. After subsequent centrifugation for 5 min at 16000*g* the supernatant was removed and stored at −20 °C. A DNAzol kit obtained from Molecular Research Center, Inc., was used to isolate *L. lactis* genomic DNA. A PCR fragment containing the coding sequence of SpaC was acquired using *B. subtilis* genomic DNA as template and a forward primer (5′-CAT GCC ATG GAA AGA GGC ACT GTA TCA A-3′) with an integrated *Nco*I site and a reverse primer (5′-CGG GAT CCT TAA ATT AAT GCT TTT GT-3′) containing a *Bam*HI site. The *nisC* PCR fragment was obtained using *L. lactis* genomic DNA as template and a forward primer (5′-CCG CTC GAG ATG AGG ATA ATG ATG AAT AAA-3′) including an *Xho*I site and a reverse primer (5′-CGG GAT CCT CAT TTC CTC TTC CCT CCT TT-3′) containing a *Bam*HI site. The PCR products were digested with the requisite enzymes and ligated into alkaline phosphatase-treated pET15b (Novagen) linearized with the same restriction enzymes. The resulting vectors encoded either the native SpaC protein (p15SC1) or an N-terminal six-histidine-tagged NisC fusion protein (p15NC1). The *spaC* and *nisC* inserts were completely sequenced by the Biotechnology Center at the University of Illinois at Urbana−Champaign.

Construction of Expression Systems for SpaC Mutants. An overlap extension PCR (OE-PCR) method was utilized to introduce the C303A mutation using purified p15SC1 as the template. Two oligonucleotide primers flanking the gene were used (forward, 727-GCACTCATACAGGGAATTAAAGTAAAGG-754; reverse, CGGGATCC(*Bam*HI)-1326-TTAAATTAAT AATGCTTTTGTCCAATC-1299) in combination with the following mutagenic primers (underlined codons encode the desired amino acid substitution): 900-TGCTTGGGCTTATGGAAGACCTGGTGTA; reverse, 916-TTCCATAAGCCCA-AGCATCTCTGCTAAA. Typical template DNA concentrations were ∼0.1−0.2 ng/mL. Two separate PCR reactions were carried out, each containing one flanking primer and one mutagenic primer. The two PCR products were purified from the agarose gel after DNA electrophoresis and used for OE-PCR reactions in which all components except the primers were combined and subjected to 5 PCR cycles, followed by addition of the outside primers and amplification over 25 additional cycles. The resulting DNA contained the correct mutation as determined by sequencing of both strands. The C349A mutation was obtained using the QuikChange kit using the protocol supplied by Stratagene using the following primers: forward, GGGGAATTTTTTCACCTACCATAGCTCATGGTTAC-AGCG; reverse, CGCTGTAACCATGAGCTATGGTAG-GTGAAAAAATTCCCC. The mutation was verified by sequencing. The OE-PCR fragment of C303A SpaC was inserted between the *Bse*RI and *Bam*HI sites of p15SC1. The resulting plasmid was treated with *Nco*I and *Bam*HI, and the excised gene was ligated into pET28a that had been digested with the same enzymes. Colonies were tested for the presence of the insert by double digest with *Nco*I and *Bam*HI. Plasmids obtained from those colonies testing positive were digested with *Bse*RI and *Xho*I and ligated into pGEX-6p1 containing *spaC* that had been digested with the same two enzymes.

Overexpression and Purification of His-Tagged NisC. To isolate the *nisC* gene product, *E. coli* strain BL21(DE3) containing p15NC1 was grown overnight in 20 mL of Luria−Bertani (LB) medium containing 100 μg/mL ampicillin (LB amp). The cells were harvested at 4750*g*, and the supernatant was decanted. The cells were resuspended in fresh LB amp (20 mL), and this suspension was used to inoculate 2 L of LB amp medium. The culture was incubated at 37 °C with agitation until the OD_{600nm} reached 1.1; then isopropyl β-D-thiogalactoside (IPTG, Acros) was added to a final concentration of 0.1 mM. The cells were grown at 25 °C for 8 h and harvested by centrifugation at 6690*g* for 15 min at 4 °C. The resulting cell paste (7.8 g) was resuspended in 23 mL of binding buffer (20 mM Tris, 5 mM imidazole, 0.5 M NaCl, pH 7.6). Hen egg white lysozyme was added to a final concentration of 0.2 mg/mL, and the mixture was frozen with liquid nitrogen and stored at −80 °C overnight.

The His-tagged (*26*) protein was isolated using a BioCAD system and a 9 × 1 cm POROS 20 metal chelate column (PerSeptive Biosystems) charged with $NiSO_4$. The lysed cell mixture was thawed at room temperature and centrifuged at 18900*g* for 30 min at 4 °C. The supernatant was filtered through a 0.45 μm syringe-tip filter and applied to the charged column at a flow rate of 3 mL/min. The following steps were carried out at a flow rate of 8 mL/min. The column was washed with binding buffer (100 mL) followed by a 30 mM imidazole buffer (20 mM Tris, 0.5 M NaCl, pH 7.6, 70 mL). The protein was eluted with a linear gradient of 30−500 mM imidazole (20 mM Tris, 0.5 M NaCl, pH 7.6, 100 mL). Fractions were monitored by UV−vis spectroscopy at 280 nm and SDS−PAGE. The fractions containing NisC were concentrated by Amicon filtration with a YM-30 ultrafiltration membrane (Millipore) and stored at 4 °C. After removal of the histidine tag by thrombin cleavage, six extra amino acids (GSHMLE) remained at the N-terminus of NisC.

For metal analysis, His_6-NisC was also purified without the use of nickel affinity chromatography. The cell paste (7.98 g) was resuspended in Tris buffer (24 mL), and hen egg white lysozyme was added to a final concentration of 0.2 mg/mL. The suspension was frozen with liquid nitrogen and stored at −80 °C. It was thawed on ice and centrifuged at 46000*g* for 30 min at 4 °C. The supernatant (27 mL) was treated with streptomycin sulfate (5% solution, 5.5 mL). The

suspension was stirred at 4 °C for 15 min and then centrifuged at 46000*g* at 4 °C for 30 min. Ammonium sulfate (10.2 g) was added to the resulting supernatant (32.5 mL, 302 mg total protein) over 15 min at 4 °C to provide a 50% saturated solution. It was stirred for an additional 15 min and then centrifuged at 46000*g* at 4 °C for 30 min.

The ammonium sulfate pellet (1.02 g) was redissolved in Tris buffer (2.25 mL) and was loaded onto a Sephadex G-25 column (Pharmacia-Biotech, 32.5 × 2.5 cm, 160 mL settled gel) previously equilibrated with Tris buffer (1 L). Fractions exhibiting a UV−vis reading >0.2 at 280 nm were pooled. A 25.5 × 2.5 cm column charged with DEAE-Sepharose Fast-Flow anion-exchange resin (Pharmacia-Biotech, 125 mL settled gel) was equilibrated with Tris buffer (1.1 L). The G-25 gel filtration product (48 mL, 145 mg total protein) was loaded directly onto the column bed. The column was washed with Tris buffer until the eluent had a negligible absorbance at 280 nm. The column was eluted with a linear NaCl gradient (0−1 M, 800 mL), and the fractions were examined using SDS−PAGE. The fractions containing His_6-NisC were combined and concentrated by Amicon filtration with a YM-30 ultrafiltration membrane (Millipore). The concentrated solution from the anion-exchange column (1.5 mL, 19 mg total protein) was loaded onto a 150 × 1.5 cm Sephacryl S-200 column (265 mL settled gel, Pharmacia-Biotech) previously equilibrated with Tris buffer containing 0.1 M NaCl (600 mL). The column was eluted with Tris buffer containing 0.1 M NaCl, and 4 mL fractions were collected. The fractions were analyzed by SDS−PAGE. Those containing His-NisC were combined and concentrated by Amicon filtration with a YM-30 ultrafiltration membrane (1.9 mg).

Cleavage of the His Tag with Thrombin. The His_6-NisC sample was incubated overnight with thrombin (10 units of thrombin protease/mg of His-NisC) at 22 °C. The resulting NisC protein was purified either by nickel affinity chromatography on a Hi-Trap column (Pharmacia, 1 mL) or by size exclusion chromatography on a Sephacryl S-200 column (150 × 1.5 cm, 265 mL settled gel).

SpaC Overexpression and Purification. For purification of recombinant SpaC, *E. coli* BL21(DE3) cells containing p15SC1 were grown overnight in LB amp at 37 °C with agitation (20 mL). The cells were sedimented, resuspended in fresh LB amp (20 mL), and then added to 2 L of LB amp. After incubation at 37 °C with agitation until the OD_{600nm} reached 1.3, IPTG was added to a final concentration of 0.3 mM. The cells were grown at 25 °C for 8 h and harvested by centrifugation at 3130*g* for 30 min at 4 °C. The cells (8.3 g) were resuspended in Tris buffer (25 mL), and hen egg white lysozyme was added to a final concentration of 0.2 mg/mL. The suspension was frozen with liquid nitrogen and stored at −80 °C.

Purification was carried out as described for the non-nickel affinity purification of His_6-NisC. The frozen suspension of cell paste was thawed on ice and centrifuged at 46000*g* for 30 min at 4 °C. The supernatant (24 mL, 151.9 mg total protein) was treated with streptomycin sulfate (5% solution, 4.5 mL), and the resulting supernatant (28 mL, 132.5 mg total protein) was brought to 50% saturation with ammonium sulfate (8.8 g). The ammonium sulfate pellet (0.4 g) was redissolved in Tris buffer (2.5 mL) and desalted on a Sephadex G-25 column (32.5 × 2.5 cm, 160 mL settled gel). The protein was purified by DEAE-Sepharose anion-exchange chromatography (25.5 × 2.5 cm, 125 mL settled gel) using a linear NaCl gradient (0−1 M) in Tris buffer. The fractions containing SpaC were combined and concentrated by Amicon filtration with a YM-30 ultrafiltration membrane (Millipore). The concentrated solution (4 mL, 5.3 mg total protein) was loaded onto a 2.5 × 41.6 cm Sephacryl S-200 column (200 mL settled gel) and eluted with Tris buffer. The fractions containing SpaC were combined and concentrated by Amicon filtration (4.5 mg).

Expression and Purification of SpaC Mutants. An overnight culture of *E. coli* BL21(DE3) cells carrying the pGEX-6p1 plasmid containing the gene sequence for C303A SpaC was grown in LB amp at 37 °C with shaking (100 mL). The cells were divided into three aliquots of 30 mL and pelleted, followed by resuspension in 1 mL of fresh LB. Each 1 mL aliquot was added to 3 L of LB amp and grown at 37 °C with shaking until the OD_{600nm} reached 1.1. Overexpression of the protein was induced by addition of IPTG to a final concentration of 1 mM, and the medium was supplemented with $ZnCl_2$ to a final concentration of 100 μM. Cells were grown at 20 °C for 20−24 h and harvested by centrifugation at 15000*g* for 20 min at 4 °C. The cells (17.2 g) were resuspended in 100 mM KCl, 10% glycerol, 20 mM HEPES, pH 7.5, 1 tablet of protease inhibitor cocktail (Boehringer-Mannheim), and 10 μg/mL DNase I (30 mL), frozen in liquid nitrogen, and stored at −80 °C.

Cells were lysed by sonication, and cellular debris was pelleted by centrifugation at 29000*g* for 45 min at 4 °C. The resulting supernatant was loaded slowly (0.5 mL/min) onto a preequilibrated glutathione−Sepharose column (Amersham Bioscience, 25 mL bed volume). The column was washed extensively with 20 mM Tris and 100 mM NaCl, pH 8.3, and the GST fusion protein was eluted with 20 mM Tris, 100 mM NaCl, and 16 mM glutathione (reduced), pH 8.3 (100 mL). Fractions containing GST mutant fusion protein were combined and treated overnight at 4 °C with Prescission protease according to Amersham protocols. Cleaved SpaC mutant was purified from GST by Q-Sepharose anion-exchange column chromatography (20 mL bed volume), eluting with a linear gradient of 100 mM to 1 M NaCl in 20 mM Tris, pH 8.3. Fractions containing SpaC mutant protein were combined and concentrated by Amicon filtration (2.6 mg).

Molecular Mass Determination. Gel filtration was carried out using a 150 cm × 1.5 cm column with Sephacryl S-200 (265 mL) as the matrix. The column was eluted using Tris buffer containing 0.1 M NaCl at a flow rate of 0.6 mL/min. The following protein standards (Sigma) were applied to the column for calibration and subsequent estimation of the native molecular masses of SpaC and NisC: blue dextran (2000 kDa, void volume), β-amylase (200 kDa), alcohol dehydrogenase (150 kDa), bovine serum albumin (66 kDa), carbonic anhydrase (29 kDa), and cytochrome *c* (12.3 kDa). Samples (2 mL) were applied in Tris buffer with 0.1 M NaCl and 10% glycerol. Fractions (4 mL) were collected, and the protein elution was followed by the absorbance at 280 nm and SDS−PAGE. In addition, the aggregation state was probed by HPLC using a Bio-Sil SEC 250-5 column (300 mm × 7.8 mm, Bio-Rad), eluting with 0.1 M sodium phosphate buffer, pH 6.8, containing 0.15 M NaCl and 0.1

M sodium azide at a flow rate of 1 mL/min. Size exclusion HPLC was performed using a Beckman Gold system (model 125 solvent module and model 166 detector), monitoring at 280 nm. A mixture of the following protein standards (25 μL) was injected for estimation of the native molecular masses of SpaC and NisC: thyroglobulin (670 kDa), IgG (158 kDa), ovalbumin (44 kDa), myoglobin (17 kDa), and vitamin B_{12} (13.5 kDa).

Inductively Coupled Plasma Mass Spectrometric (ICP-MS) Analysis. All flasks and beakers were prerinsed with 20% HNO_3 and Millipore water. Dialysis was performed using slidealyzers (Pierce) presoaked in Tris buffer containing 10 g/L Chelex-100 (Bio-Rad), in the Na^+ form, to remove divalent cations. The standard enzyme preparation involved dialysis or Centricon centrifugal filtration. Dialysis was carried out with four changes of Tris buffer (1:1000), with 25−50 g/L Chelex-100 in the beaker, over a total time of 48 h at 4 °C. Centrifugal filtration was performed with Tris buffer (1:10, pretreated with 50 g/L Chelex) with at least four changes of buffer. Samples were frozen with N_2(l) and analyzed at the University of Michigan Department of Geological Sciences to determine the metal content by inductively coupled plasma mass spectrometry (ICP-MS).

PAR and DTNB Assays. The zinc content was also determined using a spectroscopic assay based on the absorption change at 500 nm associated with the formation of a zinc complex with 4-(2-pyridylazo)resorcinol (PAR, Sigma). The procedure used is a variation of the protocol used by Hunt et al. (*27*). Prior to the assay, adventitious metals were removed from both SpaC and NisC by extensive dialysis as described above, and the buffers were pretreated with 50 g/L Chelex-100. Freshly dialyzed protein solutions of SpaC and NisC tested negatively for adventitious Zn^{2+} using 0.1 M PAR. The protein-bound zinc was released by denaturation and addition of the thiol-modifying reagent 5,5′-dithiobis-(2-nitrobenzoic acid) (DTNB, Acros). The reactions were performed in 20 mM Tris, pH 7.5, with 4 M guanidine hydrochloride (Gdn-HCl). The metal assays contained approximately 9 μM SpaC or NisC in 20 mM Tris, 4 M Gdn-HCl, and 0.1 M PAR, pH 7.5, and were titrated with 1 mM DTNB in the same buffer to release all cysteine-bound metal (0−82 μM DTNB). The assays were performed at room temperature, and the titrant was added using plastic pipet tips to avoid contamination by metal syringe needles. The absorbance at 500 nm was measured, and the titration was judged to be complete when no further significant change was observed. The concentration of Zn^{2+} was determined using a standard curve prepared by dilutions of a zinc atomic absorption standard (0.0−15.3 μM). Background absorbance at 500 nm due to the minimal increase upon addition of DTNB was determined using an identical titration of a sample of the protein lacking the PAR reagent. The control values observed were subtracted from the experimental value detected with PAR.

The absorbance readings at 412 nm obtained by the addition of DTNB to samples lacking PAR were recorded and used to estimate the number of free cysteine residues in each enzyme. The titrations were judged to be complete when no further significant change at 412 nm was observed and an excess of DTNB over the theoretical number of cysteines in each protein had been added. The concentration of 2-nitro-5-thiobenzoate anions released on reaction with reduced thiol groups on the protein was determined using a standard curve that was prepared using fresh dilutions of β-mercaptoethanol (Aldrich, 0.0−15.3 μM).

Synthesis of a Dehydropeptide as Substrate for SpaC. The linear total synthesis of a dehydropeptide corresponding to residues 2−32 of the substrate for SpaC (SKFDDFDLDV-VKVSKQDSKITPQWKDhaEDhaLCA) was conducted in two steps. A peptide containing phenylselenocysteine at positions 26 and 28 was performed on Wang resin using standard Fmoc SPPS protocols with HBTU in NMM/DMF for the coupling steps (*20*). The HPLC trace of the resulting crude peptide mixture (0.144 g) was complex, and a number of peptide species were present as determined by MALDI-MS, with the desired mass the most abundant peak, followed closely by an M-71 peak, presumably formed by premature elimination of one of the phenylselenides and subsequent Michael addition of a piperidine molecule used in the Fmoc deprotection steps. After purification by reverse-phase (RP) HPLC on a preparative Vydac C-18 column [MALDI-LRMS *m*/*z* calcd for $(M + 1)^+$ 3823.7, found 3823.9], the cysteine residue was protected as the ethyl disulfide by reaction of the peptide (8 mg) with 5.2 μmol of 2-benzothiazole ethyl disulfide (*28*) in a mixture of water (0.131 mL) and ethanol (0.131 mL) [MALDI-LRMS *m*/*z* calcd for $(M + 1)^+$ 3883.7, found 3884.0]. The overall yield of the peptide synthesis including cysteine protection was 0.3%. The purified peptide was dissolved in a mixture of acetonitrile (20 μL) and water (20 μL), and an aqueous solution of H_2O_2 (3%, 1 μL) was added. After being stirred for 1 h at 25 °C, another aliquot of aqueous H_2O_2 (3%, 2 μL) was added. After an additional 30 min, the reaction was diluted with 1:1 acetonitrile:water, and the target dehydropeptide was purified by analytical RP-HPLC [MALDI-LRMS *m*/*z* calcd for $(M + 1)^+$ 3566.7, found 3570.0]. The peptide was then incubated with SpaC in the presence of TCEP to reduce the ethyl disulfide protecting group on the cysteine. The reaction was followed by HPLC, and a new peak with identical mass as the substrate was observed that was attributed to a cyclization product. However, the rate of its formation was identical to control reactions in the absence of enzyme.

X-ray Absorption (XAS) Data Collection and Analysis. XAS data were collected at the Stanford Synchrotron Radiation Laboratory (SSRL) on beam lines 7.3 (BL 7.3) and 9.3 (BL 9.3) operating at 3.0 GeV with beam currents between 100 and 50 mA. Si220 monochromators with 1.2 mm slits were used to provide monochromatic radiation in the 9.431−10.517 keV energy range. Harmonic rejection was achieved either by detuning the monochromator 50% at the end of the scan (10517 eV, BL 7.3) or by means of a rhodium-coated mirror with a cutoff of 13 keV placed upstream of the monochromator (BL 9.3). The protein samples were measured as frozen glasses in 20−30% ethylene glycol at 11−14 K in fluorescence mode using either a 13-element (BL 7.3) or 30-element (BL 9.3) Ge detector. On BL 7.3 the count rate of each detector channel was kept below 110 kHz while the rise in fluorescent counts through the edge was kept below 20 kHz per channel. Count rates were linear over this range, and no dead-time correction was necessary. On BL 9.3 a Soller slit assembly fitted with a 6 μ Cu filter was used in conjunction with the 30-element detector to decrease the elastic scatter peak and protect against detector saturation. Here, maximum count rates per

channel did not exceed 40 kHz. The summed data for each detector channel were then inspected, and only those channels that gave high-quality backgrounds free from glitches, drop outs, or scatter peaks were included in the final average. Data analysis was performed as previously described in detail (*29*, *30*). First, a blank data file collected under identical conditions and detector geometry was subtracted from the summed experimental data. This procedure removed any residual Cu Kβ fluorescence from the Cu filter which was still present in the detector window and produced a flat preedge close to zero. Background subtraction was carried out using the PROCESS module of EXAFSPAK (*31*) using a Gaussian preedge and fourth-order spline fit with k^4 weighting in the postedge region (spline range 9665−10517.7 eV, spline points 9665, 9949, 10233, 10517 eV). The E_0 (start of the EXAFS) was chosen as 9665 eV, and the k^3-weighted data were Fourier transformed over the range $k = 2.11-15.04$ Å^{-1}. Simulations (including the calculations of phases and amplitudes) were performed by curve fitting using the program EXCURVE (curved-wave small atom approximation) (*32*) as previously described (*29*, *30*). This allowed for inclusion of multiple scattering pathways between the zinc center and the atoms of imidazole rings of histidine residues. Parameters refined in the fits were coordination numbers, distances, and Debye−Waller (DW) factors for Zn−ligand interactions. Zn−histidine outer shell pathways were initially set at values typical for Zn−imidazole complexes (Cambridge Data Bank) but were allowed to vary from these values up to a maximum of ±0.15 Å^{-1}. E_f, a small correction to the threshold energy E_0, was also refined but was constrained to take the same value for all shells of scatterers. The amplitude reduction factor was set at 0.90. The goodness of fit was judged by a fitting parameter, F, defined as

$$F^2 = \frac{1}{N}\sum_{i=1}^{n} k^6(\text{data}_i - \text{model}_i)^2$$

where N is the number of data points.

RESULTS

Cloning and Isolation of SpaC and NisC. The *spaC* and *nisC* genes were amplified by PCR of genomic DNA isolated from *B. subtilis* and *L. lactis*, respectively. Two sequences have been reported for *spaC* which differ by 5 base pairs (*14*, *24*). The sequence that was cloned here matches that reported by Hansen and co-workers (GenBank accession number M83944). Similarly, two sequences have been reported for *nisC*, one of which is shorter by the first 12 base pairs (*33*). The gene cloned from *L. lactis* ATCC 11454 in this work included these 12 base pairs, and the sequence agreed with that determined by Engelke et al. (*15*) (accession number Z18947). The *Nco*I and *Bam*HI cloning sites of pET15b were used for insertion of the *spaC* gene, resulting in expression of the native SpaC protein. The *nisC* gene was inserted into the *Xho*I and *Bam*HI cloning sites, resulting in the expression of an N-terminal histidine-tagged fusion protein. Using this construct, six extra amino acids (GSHMLE) remain at the N-terminus of NisC after removal of the His_6 tag with thrombin. Both the *spaC* and *nisC* gene products were heterologously expressed in *E. coli* as soluble proteins at 25 °C and low IPTG concentrations.

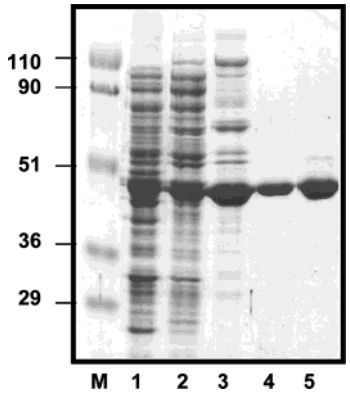

FIGURE 3: Purification of SpaC: M, low-range marker; lane 1, cell supernatant; lane 2, $(NH_4)_2SO_4$ pellet; lane 3, partially purified SpaC after DEAE anion exchange; lane 4, SpaC after S200 gel filtration; lane 5, as in lane 4 but at a higher load.

SpaC was purified using successive anion-exchange and gel filtration chromatographic steps in a final yield of 2 mg/L of cell culture (Figure 3). His_6-NisC was obtained by Ni^{2+}-(NTA) affinity chromatography providing highly purified protein. The overexpression level of His_6-NisC was considerably lower than observed with SpaC, resulting in limited quantities of protein. The molecular weights of the recombinant proteins determined by mass spectrometry were in good agreement with the theoretically calculated values (SpaC, ESI-LRMS *m*/*z* calcd 49353; found 49353 ± 49; His-NisC, MALDI-LRMS *m*/*z* calcd 50338; found 50344 ± 50; GSHMLE-NisC, MALDI-LRMS *m*/*z* calcd 48586; found 48577 ± 49). Moreover, the identity of SpaC was verified by N-terminal Edman degradation. The aggregation state of each purified recombinant enzyme was assessed by gel filtration chromatography. All three proteins (SpaC, His_6-NisC, and NisC) eluted from a Sephacryl S-200 column with a retention time consistent with a monomer. Furthermore, the samples were analyzed by HPLC and compared to standard samples confirming the monomeric form of the proteins.

Metal Content of SpaC and NisC. The proteins expressed in cells grown on unsupplemented media were analyzed for metal content using ICP-MS (see Materials and Methods). The results revealed that SpaC contained zinc with a stoichiometry of 0.64, and NisC purified without using Ni^{2+}-(NTA) affinity chromatography contained zinc with a stoichiometry of 0.61. Supplementation of the growth medium for bacteria expressing SpaC increased the zinc content of the protein to 0.84 equiv. No significant amounts of other metals were detected in these experiments, and the measured levels of zinc in the buffer used for the experiment were essentially negligible. A spectrophotometric assay using the metallochromic indicator PAR was used subsequently to verify the metal content (*27*). In the absence of denaturant, metal ions could not be detected, suggesting that PAR by itself cannot extract zinc from either SpaC or NisC. After treatment with guanidine hydrochloride and DTNB to trap reactive cysteines as disulfides, formation of the orange Zn-$(PAR)_2$ complex was observed. For quantitative experiments, the reactions were carried out with 0.1 M PAR and 8−9 μM protein. Under these conditions (pH 7, 0.1 M PAR, <12 μM Zn), over 98% of the zinc is in the 1:2 Zn:PAR complex (*27*). The color change was immediately visible upon mixing the solutions, and the initial absorbance at 500 nm increased

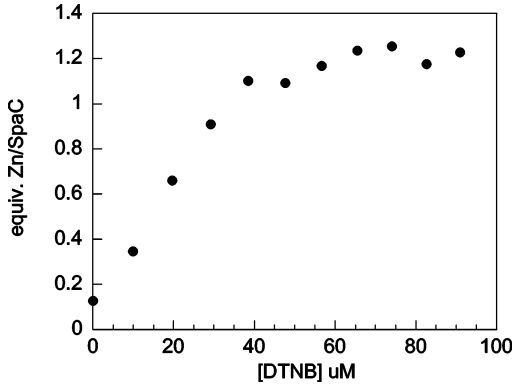

FIGURE 4: Spectroscopic estimation of zinc content of SpaC as established by a PAR assay in the presence of Gdn-HCl and DTNB (see text).

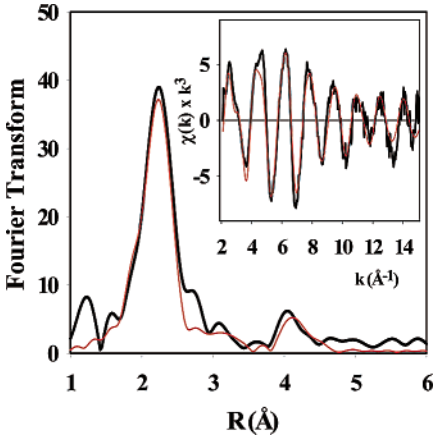

FIGURE 5: Fourier transform and EXAFS (inset) of the Zn center in SpaC. The Fourier transform (phase-corrected) was calculated from k^3 data extending from $k = 2.11-15.04$ Å^{-1}. The experimental data are depicted by thick black lines, while the simulation corresponding to 2Zn−S at 2.28 ± 0.005 Å and 2Zn−N/O at 2.01 ± 0.01 Å is shown by thin red lines.

only slightly thereafter over a period of hours. As shown in Figure 4, addition of DTNB released 1.2 equiv of zinc per SpaC polypeptide. Release of 0.86 equiv of zinc was observed per NisC polypeptide (data not shown). A higher zinc content determined by the colorimetric method compared to ICP-MS analysis has been observed previously for other zinc proteins (*34*, *35*).

Probing the Presence of Cysteine Disulfides in SpaC and NisC. After denaturation with guanidine hydrochloride in the absence of PAR, treatment of the enzymes with DTNB resulted in an increase in the absorbance at 412 nm. The concentration of free thiol in the proteins was determined using either the extinction coefficient for liberated 2-nitro-5-thiobenzoate (13600 M^{-1} cm^{-1}) or a calibration curve generated from the reaction of DTNB with β-mercaptoethanol with both methods giving similar values. Addition of excess DTNB released 8.5 ± 0.6 equiv of 2-nitro-5-thiobenzoate per SpaC, in reasonable agreement with the seven cysteines in the SpaC sequence. Using the same procedure with NisC released 3.6 equiv of 2-nitro-5-thiobenzoate. NisC possesses six cysteine residues, which suggests that the purified protein contains one disulfide.

XAS Analysis of SpaC. Two independent data sets were collected on different samples, one on BL 7.3 extending to $k = 15$ Å^{-1} and the second on BL 9.3 extending to 12.8 Å^{-1}. Both gave superimposable results. The Zn K-edge EXAFS and Fourier transform for the BL 7.3 data set are shown in Figure 5. Intense oscillations are seen in the EXAFS out to $k = 15$ Å^{-1} together with a first shell peak in the transform at $R = \sim 2.3$ Å (phase corrected). This pattern is typical of metal−thiol coordination. Given the evidence for two absolutely conserved cysteine residues and two conserved histidine residues (see Discussion), we chose a $Zn(Cys)_2(His)_2$ model for initial EXAFS simulations. Unfiltered EXAFS data were used in these fits, with multiple scattering contributions from imidazole C_β (C2/C5) and C_γ/N_γ (N3/C4) outer shell interactions. This combination of scatterers gave an excellent fit to the data, with a shell of two imidazoles at 2.01 ± 0.01 Å and a shell of two sulfur atoms at 2.28 ± 0.005 Å. The Debye−Waller (DW) terms for the Zn−S shell ($2\sigma^2 = 0.005 \pm 0.001$ Å^2) are normal for thiol ligands in the first coordination sphere of a metal ion (*36*) and suggest that the Zn center is indeed coordinated by two cysteines. The DW terms for the histidine shell ($2\sigma^2 = 0.008 \pm 0.002$ Å^2) are elevated somewhat relative to typical values for first shell scatterers (*36*, *37*), which may either suggest some heterogeneity in Zn−N(imid) bond length or the presence of a non-histidine O/N scatterer.

EXAFS studies on members of the family of Zn−thiol-containing alkyl transferase enzymes have shown a variety of coordinations ranging from $Zn-S_4$ (*38*) and $Zn-S_3(O/N)$ (*39*) to $Zn-S_2(O/N)_2$ (*40*−*42*), where one of the O/N ligands is replaced by the thiol substrate to generate a $Zn-S_3(O/N)$ environment upon substrate binding. The tetrahedral Zn site of the metalloregulatory protein SmtB exhibits $Zn-S(O/N)_3$ coordination with some evidence for a carboxylate ligand (*43*), while the *E. coli* Zn sensor Zur contains two Zn binding sites with $ZnS_3(O/N)$ and $Zn(O/N)_3$ environments, respectively (*44*). Thus every combination of S and N/O coordination is represented in Zn biochemistry. In the case of SpaC, it seems likely that Zn is ligated by two cysteine residues, but the identity of the accompanying O/N ligands is less certain.

With the above systems as background information, further simulations were carried out with the aim of limiting the possibilities for the identity of the N/O shell. The approach used was to generate fitting surfaces and/or contour maps of the goodness of fit parameter *F* versus coordination numbers of both the cysteine and O/N shells, with DW terms fixed at physically reasonable values for first shell scatterers ($2\sigma^2 = 0.005$ Å^2). For this analysis we used the $k = 15$ Å^{-1} BL 7.3 data since the extended data range would provide better resolution between Zn−S and Zn−O/N shells (*36*). With DW terms of the first shell held constant, variation of the S and N/O coordination numbers over a continuous range between 1 and 3 generates the surface shown in Figure 6A, with the contour map (equivalent to the projection of the surface on the *xy* plane) shown in Figure 6B. Inspection of these three-dimensional maps indicates that the S coordination number is extremely well-defined at 2 (2.143 at the minimum). The N/O coordination number is less well defined, however, corresponding to a shallower minimum at 1.86. When the N/O shell was further refined against its DW factor (with the S shell coordination held at 2.0), the coordination number again minimized around 2.0, but the shell could tolerate a broader range of both occupancy (1.5−2.5) and DW (0.005−0.02 A^2) (Figure 6C,D). This analysis

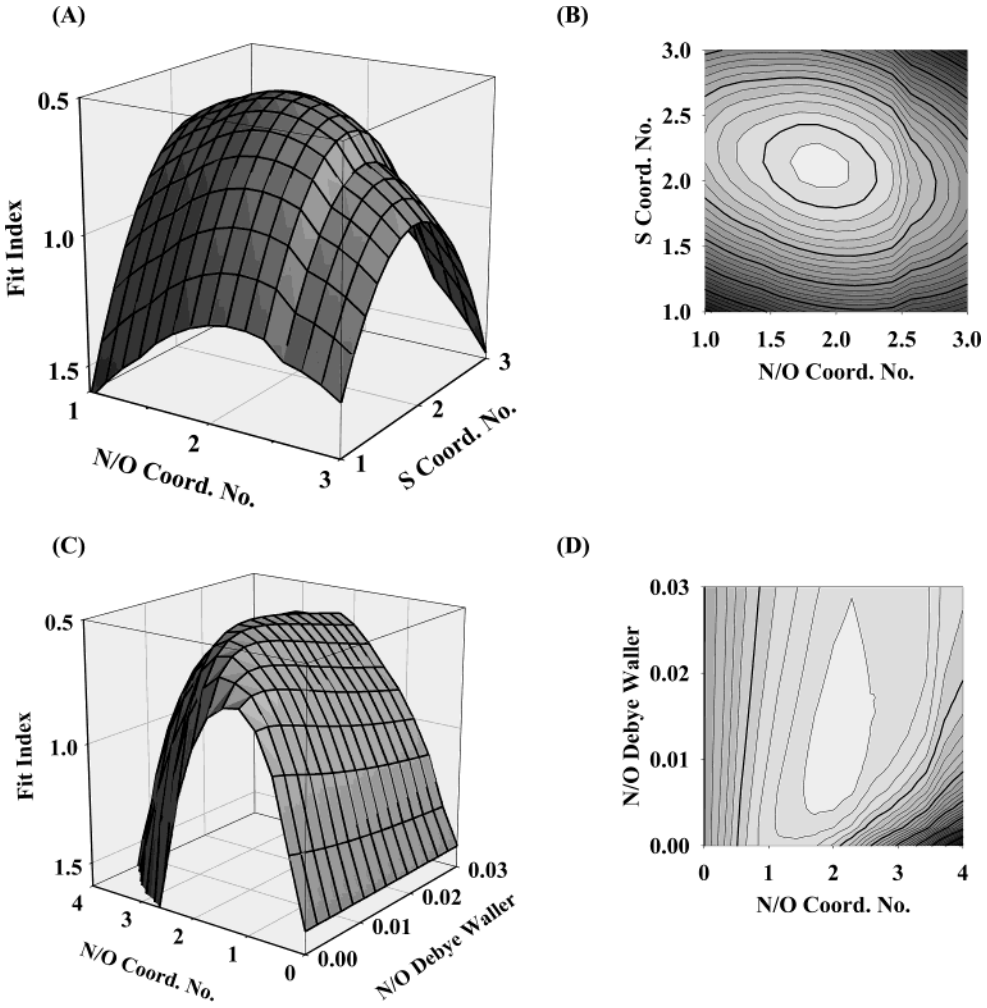

FIGURE 6: Surfaces and contour maps of metrical parameter space versus goodness of fit parameter *F*. (A) Surface generated by variation of Zn−S coordination number (1.0−3.0) against Zn−N/O coordination number (1.0−3.0). Debye−Waller factors ($2\sigma^2$) were fixed at 0.005 Å^2. (B) Contour map representing the projection of the surface of panel A onto the *xy* plane. The minimum in the map ($F = 0.542$) occurs at 2.143 Zn−S and 1.857 Zn−N/O scatterers. (C) Surface generated by variation of Zn−N/O coordination number (0−4.0) against Zn−N/O Debye−Waller factor (0−0.03 Å^2) with Zn−S coordination (Debye Waller) fixed at 2.0 (0.005 Å^2). (D) Contour map generated by projection of the surface of panel C onto the *xy* plane. The minimum in the map ($F = 0.517$) occurs at 2.29 Zn−N/O scatterers, DW = 0.013 Å^2.

shows that the EXAFS amplitudes are dominated by the more intense S shell, and accordingly, it not possible to unambiguously define the number of N/O (imidazole/water/carboxylate ligands). However, for all fits, *F* is a minimum at ~2 N/O scatterers per zinc. A zinc site composed of 2Zn−S at 2.28 Å and 2Zn−N/O is thus fully consistent with the data.

The above analysis is broadly in line with the findings of Penner-Hahn and co-workers (*36*) regarding the ability to use XAS to define coordination numbers in a mixed S/N/O environment and illustrates a general property of EXAFS methodology: distances are determined to a much higher accuracy than coordination numbers. Bond valence sum analysis (BVS) (*45*−*48*) provides a method of correlating this accurate distance information with the less precise coordination numbers, using an empirical relationship derived from crystallographic data on the wide variety of model complexes tabulated in the Cambridge Structural Database. The BVS of a metal complex is defined by the equation

$$\mathrm{BVS} = \Sigma_i \exp[(r_{0,i} - r_i)/0.37]$$

where r_i is the experimentally determined metal−ligand distance for shell *i* and $r_{0,i}$ is an empirical value, which has been determined for the *i*th metal−ligand pair such that the valence of the metal ion is satisfied. For Zn(II) the bond valence sum must equal its oxidation state of 2; hence the sum of contributions for the 2Zn−S and 2Zn−N/O contributions must equal 2. Using r_0 values of 2.09 and 1.74 for Zn−S and Zn−N/O shells, respectively (*37*, *46*, *47*), we calculate a BVS of 2.16 for the EXAFS-derived coordination site. The fact that the calculated value is above 2 suggests that the valence of the Zn ion is more than satisfied by the two sulfur and two N/O ligands at their respective distances and argues against higher coordination numbers for the N/O shell. Unfortunately, the accessible quantities of purified protein were insufficient for XAS analysis of NisC.

Zinc Content and EXAFS of SpaC Mutants. To further investigate the ligand environment of the zinc in SpaC, two mutants of the two conserved cysteines were generated, C349A and C303A. These proteins were expressed poorly and showed low solubility using the pET system used for wild-type SpaC. Expression as a fusion protein to glutathione *S*-transferase (GST) resulted in improved expression and allowed purification of the proteins. The GST fusion was

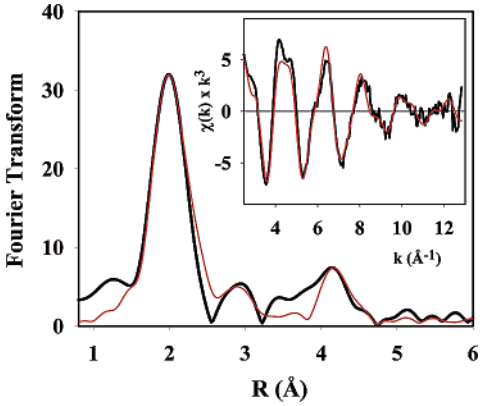

FIGURE 7: Fourier transform and EXAFS (inset) of the Zn center in C349A SpaC. The experimental data are depicted by thick black lines, while the simulation corresponding to 1Zn−S at 2.28 ± 0.01 Å, 2Zn−N(His) at 2.02 ± 0.01 Å, and 1Zn−O at 1.91 ± 0.01 Å is shown as thin red lines.

removed by proteolysis of the linker connecting the two proteins with prescission protease, and after additional chromatographic steps (see Materials and Methods) the mutants were obtained in high purity (>95%). ICP-MS analysis of both mutants indicated that they contained reduced amounts of Zn, 0.2−0.3 equiv per mutant polypeptide.

A 260 μM sample of C349A was analyzed by EXAFS to determine whether the spectrum was consistent with the loss of a coordinated cysteine residue. Experimental and simulated FT and EXAFS for the mutant are shown in Figure 7 and show a significant reduction in the intensity of the first shell in the FT and the EXAFS oscillations, consistent with the loss of scattering from a Zn−S interaction. The mutant spectrum was analyzed using the WT parameters as a starting parameter set. When the sulfur shell coordination number and DW factor were allowed to float freely, the model refined to 1.2 S with a DW term ($2\sigma^2$) of 0.012 Å^2. This DW term is large for a first shell scatterer. When the DW term was fixed at 0.005 Å^2 (the value determined for the Zn−S shell of the WT protein), the Zn−S coordination number refined to 0.8. In both of these fits an additional low *Z* scatterer was required to reproduce the EXAFS and FT amplitudes. The best fit using integral coordination numbers ($F = 0.596$) is shown in Figure 7, with 2Zn−N(His) at 2.02 Å ($2\sigma^2 = 0.002$ Å^2), 1Zn−S(Cys) at 2.28 Å ($2\sigma^2 = 0.009$ Å^2), and 1 low *Z* scatterer (O/N) at 1.91 Å ($2\sigma^2 = 0.009$ Å^2). These data provide strong evidence that C349 is a ligand to Zn and that in the mutant it is either replaced by solvent or that some other O- or N-donor from a protein residue is recruited to replace the zinc−thiol interaction. In this regard, fits employing 3Zn−His and 1Zn−Cys interactions were statistically equivalent to the fit shown in Figure 7.

Unfortunately, C303A was not amenable for EXAFS analysis as the protein proved unstable upon concentration leading to precipitation. Samples of C303A at lower concentration (100 μM) were not useable for XAS analysis.

DISCUSSION

The biosynthesis and mode of action of lantibiotics have been extensively investigated for several decades. Despite the cloning of the entire biosynthetic gene clusters for several family members, the details of the posttranslational modifications are unclear, and in vitro reconstitution has remained elusive. Genetic investigations have given a basic picture of the events involved (Figure 2) but have not provided insight into the mechanism by which these transformations occur. Yeast two-hybrid assays and coimmunoprecipitation studies have suggested that SpaC and NisC are present as part of a multienzyme complex with the dehydratases SpaB and NisB and the ABC transporters SpaT and NisT. The two-hybrid studies also suggest that SpaC and NisC undergo self-association in vivo (*49*, *50*). Our observations with heterologously expressed and purified proteins indicate that the SpaC and NisC are monomers in solution, suggesting that for these recombinant proteins any self-association is weak. In lantibiotic-producing strains these interactions may be enforced by oligomerization with the other components of the multienzyme complex. In fact, ABC transporters are usually dimeric (*51*, *52*) and may provide a membrane anchor that results in a complex that involves multiple LanC proteins. The enzymatic activity of neither SpaC nor NisC can be addressed at present because the putative substrates for the cyclase enzymes are 56−57 amino acid peptides containing the unnatural dehydroamino acids Dha and Dhb. They cannot be directly accessed by bacterial expression, and to date no in vitro activity has been reported for the dehydratase (LanB) enzymes (*15*, *17*, *53*), the catalysts that generate the substrates for the cyclases (*16*, *54*). In this work, we tested the cyclase activity with a synthetic truncated substrate representing SpaS2−33 prepared by Fmoc-based solid-phase peptide synthesis using the methodologies we developed previously for preparation of dehydropeptides (see Materials and Methods) (*20*, *21*). This peptide contained two Dha residues at positions 26 and 28 and a cysteine at position 30 and served as a potential substrate for the formation of the A-ring of subtilin. Unfortunately, no cyclization activity could be detected with SpaC above background. This lack of activity could be due to the substrate being a truncated version of the true substrate or because other components of the multimeric lantibiotic synthetase were absent.

Despite the inability to demonstrate cyclization activity, our characterization of the SpaC and NisC proteins provides the first clues as to how the dehydrated peptide substrate may be activated toward intramolecular nucleophilic addition. As evidenced by the spectrophotometric assays, both proteins contain a stoichiometric amount of zinc. The ICP experiments provide levels of 0.6−0.7 equiv of zinc for protein purified from cells grown on unsupplemented medium. These levels are comparable with those reported for several other zinc enzymes with cysteine ligands including methylcobamide: coenzyme M methyltransferase (0.8 equiv) (*55*), cobalamin-independent methionine synthase (0.7 equiv) (*56*), and cobalamin-dependent methionine synthase (0.7−0.8 equiv) (*57*). The zinc in SpaC and NisC could provide structural integrity or act as a Lewis acid for the electrophilic activation of a carbonyl group (*58*). Although we cannot rule out a structural role for zinc in the LanC enzymes nor that it activates the carbonyl of Dha and Dhb residues, our results in combination with studies on other proteins suggest that the metal may instead activate the cysteine residues for Michael addition to the dehydroamino acids.

An increasing number of enzymes catalyzing S-alkylation reactions have been found to contain zinc ions in their active sites, including the prototypical Ada protein (*59*, *60*), the

```
SpaC    210 QFTDIEKKAY PYGNFNMGLA HGIPGPICVL SSALIQGIKV KGQEAAIEKM ANFLLEFSEK 269
EpiC    228 QFLDIDKQNF PSGNINLGLA HGILGPLSLT ALSKMNGIEI EGHEEFLQDF TSFLLKPEFK 287
NisC    192 QMSQSESEMY PLGCLNMGLA HGLAGAGCIL AYAHIKGYSN EASLSALQKI IFIYEKFELE 251
PepC    184 IKFNNDDYLL DTILSNLGYA HGIPGIINTL CNSYKRGYGI IKTKKILEQS IFTLLQNLKL 243
                          * * * **  *           *

SpaC    270 EQDSLFWKGI ISFEEYQYGS PPNAVNFSRD AWCYGRPGVC LALVKAGKAL QNTELINIGV 329
EpiC    288 NNNEWFDR-- --YDILENYI PNYSV---RN GWCYGDTGIM NTLLLSGKAL NNEGLIKMSK 340
NisC    252 IKNQFLWKDG LVADELKKEK VIREASFIRD AWCYGGPGIS LLYLYGGLAL DNDYFVDKAE 311
PepC    244 ENGTIYIP-- ---------N DIESPNDYRD AWCYGLPSVA YTIFNVSSTL KNKSLIELSE 292
                                        *   ****               *  *

SpaC    330 QNLRYTISDI RG---IFSPT ICHGYSGIGQ ILLAVNLLTG QEYFKEELQE IKQ---KIMS 383
EpiC    341 NILINIIDKN NDD--LISPT FCHGLASHLT IIHQANKFFN LSQVSTYIDT IVR---KIIS 395
NisC    312 KILESAMQRK LG---IDSYM ICHGYSGLIE ICSLFKRLLN TKKFDSYIEE FNVNSEQILE 368
PepC    293 SLLHQVFLRS DNATKLISPT LCHGFSGVVM ISLLMNNNEL SSKYQK---- ------KIIQ 342
              *               *    ***       *                          *
```

FIGURE 8: Sequence alignment of conserved areas of several LanC proteins: PepC, putative cyclase involved in Pep5 biosynthesis, and EpiC, putative cyclase involved in epidermin biosynthesis.

cobalamin-dependent and -independent methionine synthases (*56*, *57*, *61*), protein farnesyltransferase (*62*−*64*), epoxyalkane:coenzyme M transferase (*65*), and methylcobamide:coenzyme M methyltransferase (*42*, *55*). The zinc in these metalloenzymes is believed to activate the thiol of their substrates by lowering the pK_a and enhancing the reactivity at neutral pH. For example, the pH dependence of the binding of the peptide substrate to farnesyltransferase indicates that the pK_a of the cysteine is lowered from 8.3 for the free peptide (GCVLS) to approximately 6.4 upon binding to the enzyme (*63*). One noticeable feature that is common among this family of enzymes is the presence of two or more cysteine residues in the zinc coordination sphere and an overall net negative charge. In the founding member of the class, the DNA repair protein Ada features a Cys_4 coordination environment resulting in a net −2 charge. One of these cysteines is highly activated for nucleophilic addition and repairs methylated DNA lesions (*59*). The cobalamin-dependent methionine synthase and betaine homocysteine transferase each contain three Cys ligands to the metal and presumably one water that is replaced by the homocysteine substrate to again provide an S_4 coordination (*57*, *66*). In cobalamin-independent Met synthase two cysteines and one histidine make up the protein ligands with the homocysteine substrate as the fourth ligand giving a net charge of −1 (*56*). Similarly, farnesyl and geranylgeranyl transferase provide a CysHisAsp coordination environment with the cysteine of the substrate displacing a water ligand during catalysis (*64*, *67*). The net negative charge of the zinc site in all these enzymes has been shown to be important in model studies, which have confirmed the increased reactivity of thiolates coordinated to an electron-rich Zn center (*68*−*75*). In these studies, the nucleophilicity of a zinc-bound thiolate was estimated to be between that of a free thiolate and a thiol (*69*, *73*). Recent mutagenesis studies on protein farnesyltransferase have also supported the importance of the net negative charge for catalysis (*76*).

The LanC proteins involved in the biosynthesis of several lantibiotics share low sequence similarity (∼20−30%, Figure 8). Only very few amino acids are strictly conserved, but these include two cysteine residues (Cys284 and Cys330, NisC numbering) and two histidines (His212 and His331) (Figure 8). These residues are also conserved in the C-terminal part of the LanM proteins (*10*, *77*). The surrounding sequence environments of these residues do not display significant homology with the metal binding ligands of any of the cysteine-rich zinc sites discussed above. However, many of the established members of this class of metalloproteins do not display sequence similarity between their respective metal binding motifs. Given the proposed role of the LanC enzymes to catalyze the Michael addition of cysteine residues onto the dehydrated peptide, it is plausible that the cysteine nucleophile is activated by zinc in analogy with other proteins catalyzing thiol alkylation. To sustain a reasonable rate of lanthionine formation at neutral pH, activation of the cysteine thiols of the substrate by deprotonation is required. For instance, the rate constant for the addition of free thiols to α,β-unsaturated centers is 10^{10}-fold smaller than observed for the corresponding thiolates (*78*). Similarly, we have found that nonenzymatic biomimetic cyclization to form the B-ring of nisin and subtilin only takes place at pH >8 (*20*, *21*). As a working model, the two conserved cysteines of the cyclase could provide two of the ligands to the metal, with the thiolate of the substrate generating the typical negatively charged zinc binding site. Our EXAFS data on wild-type SpaC and the C349A mutant are fully consistent with two sulfur ligands to the zinc in the former and just one thiolate ligand in the latter. These studies also indicate two other N/O ligands in wild-type SpaC that may be two conserved histidines, but their identity is less well defined. In the zinc−thiolate proteins discussed above, the coordination number in the catalytically active form of the protein is 4. Hence either the substrate would have to replace one of the two histidine ligands or the coordination environment of the resting enzyme involves 2 Cys, 1 His, and one other ligand, possibly water. At present, we have been unable to test the binding of substrate to NisC or SpaC as the full-length dehydrated peptide is not available.

If only one of the two conserved His residues serves as metal ligand, the second His could function as a base to deprotonate the cysteine of the substrate *or* to protonate the enolate formed upon conjugate addition (e.g., Scheme 1 for the formation of the B-ring of subtilin and nisin). It should be noted that because of the *anti* stereochemistry of the addition of the cysteine to the *Si*-face of the dehydroamino acid and the subsequent protonation of the enolate from the opposite face, the conserved His cannot fulfill the role of both active site base and acid. Interestingly, in the past two years, several reports have shown that mammalian erythrocytes from human and mouse contain proteins that show high homology with the LanC proteins (*81*−*84*). These proteins, the function of which is currently unknown, have been

Scheme 1

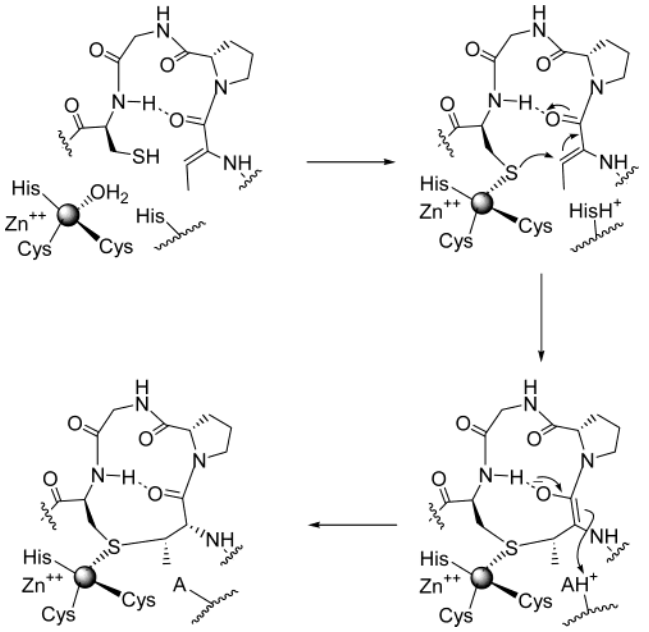

designated the generic name LANCL for LanC-like proteins and are expressed in high levels in testis and brain. Given the conserved putative metal binding residues, we speculate that these proteins are involved in alkylation of thiol substrates.

Clearly, other roles for the zinc center in NisC and SpaC can be proposed, including activation of the carbonyl of the α,β-unsaturated centers. However, coordination to the carbonyl electrophile during the alkyl group transfer seems difficult for the formation of the smaller lanthionine rings. It has been shown in NMR studies that the four amino acid B-ring present in both nisin and subtilin attains a β-turn conformation in which the N−H of the cysteine residue is hydrogen bonded to the carbonyl of the dehydrobutyrine (Scheme 1) (*85*−*88*). It is likely that this interaction is also present in the transition state for ring formation and metal coordination to the central carbonyl appears difficult, although not impossible. Whether the substrate indeed binds to the zinc site or whether the metal fulfills a structural role such as that observed recently in the McbB protein involved in the biosynthesis of microcin B17 (*35*) remains to be determined in future studies.

ACKNOWLEDGMENT

Mass spectra were recorded on a Voyager mass spectrometer funded in part by the National Institutes of Health (Grant RR 11966). We gratefully acknowledge the use of facilities at the Stanford Synchrotron Radiation Laboratory, which is supported by the National Institutes of Health Biomedical Research Technology Program, Division of Research Resources, and by the U.S. Department of Energy, Basic Energy Sciences (BES) and Office of Biological and Environmental Research (OBER).

REFERENCES

1. van Kraaij, C., de Vos, W. M., Siezen, R. J., and Kuipers, O. P. (1999) *Nat. Prod. Rep. 16*, 575−587.
2. Sahl, H. G., and Bierbaum, G. (1998) *Annu. Rev. Microbiol. 52*, 41−79.
3. Schnell, N., Entian, K.-D., Schneider, U., Götz, F., Zahner, H., Kellner, R., and Jung, G. (1988) *Nature 333*, 276−278.
4. Nissen-Meyer, J., and Nes, I. F. (1997) *Arch. Microbiol. 167*, 67−77.
5. Ruhr, E., and Sahl, H. G. (1985) *Antimicrob. Agents Chemother. 27*, 841−845.
6. Breukink, E., Wiedemann, I., van Kraaij, C., Kuipers, O. P., Sahl, H., and de Kruijff, B. (1999) *Science 286*, 2361−2364.
7. Wiedemann, I., Breukink, E., van Kraaij, C., Kuipers, O. P., Bierbaum, G., de Kruijff, B., and Sahl, H. G. (2001) *J. Biol. Chem. 276*, 1772−1779.
8. Breukink, E., van Heusden, H. E., Vollmerhaus, P. J., Swiezewska, E., Brunner, L., Walker, S., Heck, A. J., and de Kruijff, B. (2003) *J. Biol. Chem. 278*, 19898−19903.
9. Ingram, L. C. (1969) *Biochim. Biophys. Acta 184*, 216−219.
10. Siezen, R. J., Kuipers, O. P., and de Vos, W. M. (1996) *Antonie van Leeuwenhoek 69*, 171−184.
11. McAuliffe, O., Ross, R. P., and Hill, C. (2001) *FEMS Microbiol. Rev. 25*, 285−308.
12. Delves-Broughton, J., Blackburn, P., Evans, R. J., and Hugenholtz, J. (1996) *Antonie van Leeuwenhoek 69*, 193−202.
13. Banerjee, S., and Hansen, J. N. (1988) *J. Biol. Chem. 262*, 9508−9514.
14. Hansen, J. N., Chung, Y. J., and Steen, M. T. (1991) *J. Bacteriol. 174*, 1417−1422.
15. Engelke, G., Gutowski-Eckel, Z., Hammelmann, M., and Entian, K.-D. (1992) *Appl. Environ. Microbiol. 58*, 3730−3743.
16. Sen, A. K., Narbad, A., Horn, N., Dodd, H. M., Parr, A. J., Colquhoun, I., and Gasson, M. J. (1999) *Eur. J. Biochem. 261*, 524−532.
17. Xie, L., Chatterjee, C., Balsara, R., Okeley, N. M., and van der Donk, W. A. (2002) *Biochem. Biophys. Res. Commun. 295*, 952−957.
18. Kupke, T., and Götz, T. (1996) *J. Bacteriol. 178*, 1335−1340.
19. Meyer, C., Bierbaum, G., Heidrich, C., Reis, M., Süling, J., Iglesias-Wind, M. I., Kempter, C., Molitor, E., and Sahl, H.-G. (1995) *Eur. J. Biochem. 232*, 478−489.
20. Okeley, N. M., Zhu, Y., and van der Donk, W. A. (2000) *Org. Lett. 2*, 3603−3606.
21. Zhou, H., and van der Donk, W. A. (2002) *Org. Lett. 4*, 1335−1338.
22. Zhu, Y., Gieselman, M., Zhou, H., Averin, O., and van der Donk, W. A. (2003) *Org. Biomol. Chem. 1*, 3304−3315.
23. Sambrook, J., Fritsch, E. F., and Maniatis, T. (1989) *Molecular cloning: a laboratory manual*, 2nd ed., Cold Spring Harbor Laboratory, Cold Spring Harbor, NY.
24. Klein, C., Kaletta, C., Schnell, N., and Entian, K.-D. (1992) *Appl. Environ. Microbiol. 58*, 132−142.
25. Kuipers, O. P., Rollema, H. S., Yap, W. M., Boot, H. J., Siezen, R. J., and de Vos, W. M. (1992) *J. Biol. Chem. 267*, 24340−24346.
26. Porath, J. (1992) *Protein Expression Purif. 3*, 263−281.
27. Hunt, J. B., Neece, S. H., and Ginsburg, A. (1985) *Anal. Biochem. 146*, 150−157.
28. Brzezinska, E., and Ternay, A. L. (1994) *J. Org. Chem. 59*, 8239−8244.
29. Blackburn, N. J., Rhames, F. C., Ralle, M., and Jaron, S. (2000) *J. Biol. Inorg. Chem. 5*, 341−353.
30. Eisses, J. F., Stasser, J. P., Ralle, M., Kaplan, J. H., and Blackburn, N. J. (2000) *Biochemistry 39*, 7337−7342.
31. George, G. N. (1995) Stanford Synchrotron Radiation Laboratory, Menlo Park, CA.
32. Binsted, N., Gurman, S. J., and Campbell, J. W. (1998) Daresbury Laboratory EXCURV98 Program.
33. Kuipers, O. P., Beerthuyzen, M. M., Siezen, R. J., and De Vos, W. M. (1993) *Eur. J. Biochem. 216*, 281−291.
34. Myers, L. C., Terranova, M. P., Nash, H. M., Markus, M. A., and Verdine, G. L. (1992) *Biochemistry 31*, 4541−4547.
35. Zamble, D. B., McClure, C. P., Penner-Hahn, J. E., and Walsh, C. T. (2000) *Biochemistry 39*, 16190−16199.
36. Clark-Baldwin, K., Tierney, D. L., Govindaswamy, N., Gruff, E. S., Kim, C., Berg, J., Koch, S. A., and Penner-Hahn, J. E. (1998) *J. Am. Chem. Soc. 120*, 8401−8409.
37. Bell, J., Ash, D. E., Snyder, L. M., Kulathila, R., Blackburn, N. J., and Merkler, D. J. (1997) *Biochemistry 36*, 16239−16246.
38. Lin, Y., Dotsch, V., Wintner, T., Peariso, K., Myers, L. C., Penner-Hahn, J. E., Verdine, G. L., and Wagner, G. (2001) *Biochemistry 40*, 4261−4271.

39. Peariso, K., Zhou, Z. S., Smith, A. E., Matthews, R. G., and Penner-Hahn, J. E. (2001) *Biochemistry 40*, 987−993.
40. Peariso, K., Zhou, Z. S., Smith, A. E., Mathews, R. G., and Penner-Hahn, J. E. (2001) *Biochemistry 40*, 987−993.
41. Zhou, Z. Z., Peariso, K., Penner-Hahn, J. E., and Mathews, R. G. (1999) *Biochemistry 38*, 15915−15926.
42. Gencic, S., LeClerc, G. M., Gorlatova, N., Peariso, K., Penner-Hahn, J. E., and Grahame, D. A. (2001) *Biochemistry 40*, 13068−13078.
43. VanZile, M. L., Cosper, N. J., Scott, R. A., and Giedroc, D. P. (2000) *Biochemistry 39*, 11818−11829.
44. Outten, C. E., Tobin, D. A., Penner-Hahn, J. E., and O'Halloran, T. V. (2001) *Biochemistry 40*, 10417−10423.
45. Brown, I. D., and Altermatt, D. (1985) *Acta Crystallogr. B41*, 244−247.
46. Brese, N. E., and O'Keeffe, M. (1991) *Acta Crystallogr. B47*, 192−197.
47. Thorp, H. H. (1992) *Inorg. Chem. 31*, 1585−1588.
48. Liu, W., and Thorp, H. H. (1993) *Inorg. Chem. 32*, 4102−4105.
49. Kiesau, P., Eikmanns, U., Gutowski-Eckel, Z., Weber, S., Hammelmann, M., and Entian, K.-D. (1997) *J. Bacteriol. 179*, 1475−1481.
50. Siegers, K., Heinzmann, S., and Entian, K.-D. (1996) *J. Biol. Chem. 271*, 12294−12301.
51. Higgins, C. F. (1992) *Annu. Rev. Cell Biol. 8*, 67−113.
52. Fath, M. J., and Kolter, R. (1993) *Microbiol. Rev. 57*, 995−1017.
53. Peschel, A., Ottenwälder, B., and Götz, F. (1996) *FEMS Microbiol. Lett. 137*, 279−284.
54. Koponen, O., Tolonen, M., Qiao, M. Q., Wahlstrom, G., Helin, J., and Saris, P. E. J. (2002) *Microbiology 148*, 3561−3568.
55. LeClerc, G. M., and Grahame, D. A. (1996) *J. Biol. Chem. 271*, 18725−18731.
56. Gonzalez, J. C., Peariso, K., Penner-Hahn, J. E., and Matthews, R. G. (1996) *Biochemistry 35*, 12228−12234.
57. Goulding, C. W., and Matthews, R. G. (1997) *Biochemistry 36*, 15749−15757.
58. McCall, K. A., Huang, C.-C., and Fierke, C. A. (2000) *J. Nutr. 130*, 1437S−1446S.
59. Myers, L. C., Terranova, M. P., Ferentz, A. E., Wagner, G., and Verdine, G. L. (1993) *Science 261*, 1164−1167.
60. Myers, L. C., Verdine, G. L., and Wagner, G. (1993) *Biochemistry 32*, 14089−14094.
61. Matthews, R. G., and Goulding, C. W. (1997) *Curr. Opin. Chem. Biol. 1*, 332−339.
62. Hightower, K. E., and Fierke, C. A. (1999) *Curr. Opin. Chem. Biol. 3*, 176−181.
63. Hightower, K. E., Huang, C. C., Casey, P. J., and Fierke, C. A. (1998) *Biochemistry 37*, 15555−15562.
64. Huang, C. C., Casey, P. J., and Fierke, C. A. (1997) *J. Biol. Chem. 272*, 20−23.
65. Allen, J. R., and Ensign, S. A. (1997) *J. Biol. Chem. 272*, 32121−32128.
66. Breksa, A. P., III, and Garrow, T. A. (1999) *Biochemistry 38*, 13991−13998.
67. Dolence, J. M., Rozema, D. B., and Poulter, C. D. (1997) *Biochemistry 36*, 9246−9252.
68. Wilker, J. J., and Lippard, S. J. (1995) *J. Am. Chem. Soc. 117*, 8682−8683.
69. Wilker, J. J., and Lippard, S. J. (1997) *Inorg. Chem. 36*, 969−978.
70. Grapperhaus, C. A., Tuntulani, T., Reibenspies, J. H., and Darensbourg, M. Y. (1998) *Inorg. Chem. 37*, 4052−4058.
71. Chiou, S.-J., Innocent, J., Riordan, C. G., Lam, K.-C., Liable-Sands, L., and Rheingold, A. L. (2000) *Inorg. Chem. 39*, 4347−4353.
72. Bridgewater, B. M., Fillebeen, T., Friesner, R. A., and Parkin, G. (2000) *J. Chem. Soc., Dalton Trans.*, 4494−4496.
73. Warthen, C. R., Hammes, B. S., Carrano, C. J., and Crans, D. C. (2001) *J. Biol. Inorg. Chem. 6*, 82−90.
74. Brand, U., Rombach, M., Seebacher, J., and Vahrenkamp, H. (2001) *Inorg. Chem. 40*, 6151−6157.
75. Chiou, S. J., Riordan, C. G., and Rheingold, A. L. (2003) *Proc. Natl. Acad. Sci. U.S.A. 100*, 3695−3700.
76. Harris, C. M., Derdowski, A. M., and Poulter, C. D. (2002) *Biochemistry 41*, 10554−10562.
77. Skaugen, M., Abildgaard, C. I., and Nes, I. F. (1997) *Mol. Gen. Genet. 253*, 674−686.
78. Bednar, R. A. (1990) *Biochemistry 29*, 3684−3690.
79. Myers, L. C., Cushing, T. D., Wagner, G., and Verdine, G. L. (1994) *Chem. Biol. 1*, 91−97.
80. Ohkubo, T., Sakashita, H., Sakuma, T., Kainosho, M., Sekiguchi, M., and Morikawa, K. (1994) *J. Am. Chem. Soc. 116*, 6035−6036.
81. Bauer, H., Mayer, H., Marchler-Bauer, A., Salzer, U., and Prohaska, R. (2000) *Biochem. Biophys. Res. Commun. 275*, 69−74.
82. Mayer, H., Bauer, H., Breuss, J., Ziegler, S., and Prohaska, R. (2001) *Gene 269*, 73−80.
83. Mayer, H., Bauer, H., and Prohaska, R. (2001) *Cytogenet. Cell Genet. 93*, 100−104.
84. Mayer, H., Pongratz, M., and Prohaska, R. (2001) *DNA Sequence 12*, 161−166.
85. Van de Ven, F. J., Van den Hooven, H. W., Konings, R. N., and Hilbers, C. W. (1991) *Eur. J. Biochem. 202*, 1181−1188.
86. Chan, W. C., Bycroft, B. W., Leyland, M. L., Lian, L. Y., Yang, J. C., and Roberts, G. C. (1992) *FEBS Lett. 300*, 56−62.
87. Lian, L. Y., Chan, W. C., Morley, S. D., Roberts, G. C., Bycroft, B. W., and Jackson, D. (1992) *Biochem. J. 283*, 413−420.
88. Goodman, M., Palmer, D. E., Mierke, D., Ro, S., Nunami, K., Wakamiya, T., Fukase, K., Horimoto, S., Kitazawa, M., Fujita, H., Kubo, A., and Shiba, T. (1991) in *Nisin and Novel Lantibiotics* (Jung, G., and Sahl, H.-G., Eds.) pp 59−75, ESCOM, Leiden, The Netherlands.

BI0354942